The Effect of Horizontal Pressure Gradients on the Momentum Transport in Tropical Convective Lines. Part II: Lagrangian Calculations

MARIA FLATAU* AND DUANE E. STEVENS

Department of Atmospheric Sciences, Colorado State University, Fort Collins, CO 80523

(Manuscript received 19 March 1986, in final form 4 February 1987)

ABSTRACT

The movement of a set of Lagrangian parcels in the two-dimensional pressure field associated with a tropical convective line is considered. The results are compared with observational characteristics of GATE quasi-two-dimensional convective lines. It is shown that for the composite, slow-moving GATE convective line it is necessary to account for horizontal pressure gradients in order to obtain realistic momentum flux. The role of vertical pressure gradients and initial conditions for an air parcel's movement is studied. Based on the results, some suggestions concerning proper formulation of parameterization of the convective momentum flux are made.

1. Introduction

Recent observational studies (LeMone, 1983; LeMone et al., 1984) show that in tropical quasi-two-dimensional convective lines, the convection-generated horizontal pressure gradients can strongly influence convective momentum fluxes. Cumulus convective parameterizations usually neglect this effect by assuming that the horizontal momentum is conserved in convective drafts. In Part I of this paper we estimated the magnitude of the error made by neglecting cloud-generated horizontal pressure forces for the two-dimensional convective lines studied by LeMone (1983) and LeMone et al. (1984) using the modified version of the Fritsch and Chappell (1980, hereafter FC) parameterization. Cloud properties in the Part I calculations were estimated from the one-dimensional, stationary cloud model that implied that updraft and downdraft were represented by a single parcel moving in the environment determined by the sounding ahead of the convective line. Since vertical velocities in the updraft and downdraft obtained with this method were much too large compared with observations, we had to use vertical velocities in drafts taken from measurements in momentum flux calculations.

In Part II of this paper we evaluate the effect of horizontal pressure gradients using a somewhat different approach. We consider a set of Lagrangian parcels moving in the two-dimensional pressure field generated by the convective line. As in Part I, we perform our calculations for the convective region of the line (i.e., for the first 30 km behind the leading edge). The environment for the moving parcels is now determined, not only by the sounding ahead of the line, but also by the two-dimensional disturbance caused by the presence of convection (LeMone, 1983). The Lagrangian parcels have different initial temperature depending on their initial position in the line. We calculate the average vertical velocity and momentum flux for all parcels and compare these results with observations (Zipser and LeMone, 1980; LeMone, 1983; LeMone and Zipser, 1980) and with the FC calculations of Part I. Because Part I has shown that the shear effects dominate in fast-moving lines, we concentrate here on the case of slow-moving convective line for which the pressure gradients have the greatest impact.

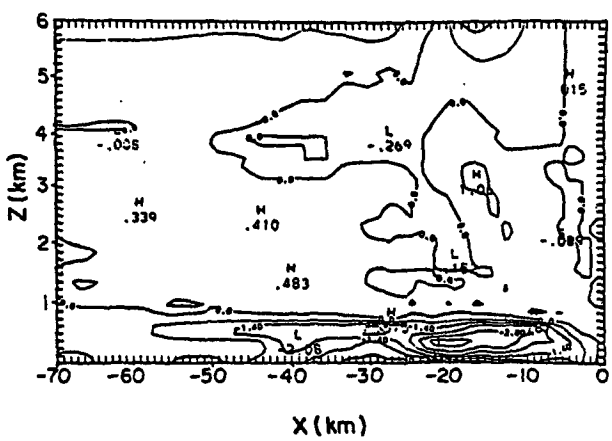

FIG. 1. Disturbance of the virtual temperature calculated from the hydrostatic equation and the pressure disturbance field for the slow GATE convective line.

* On leave from the Institute of Meteorology and Water Management, Warsaw, Poland.

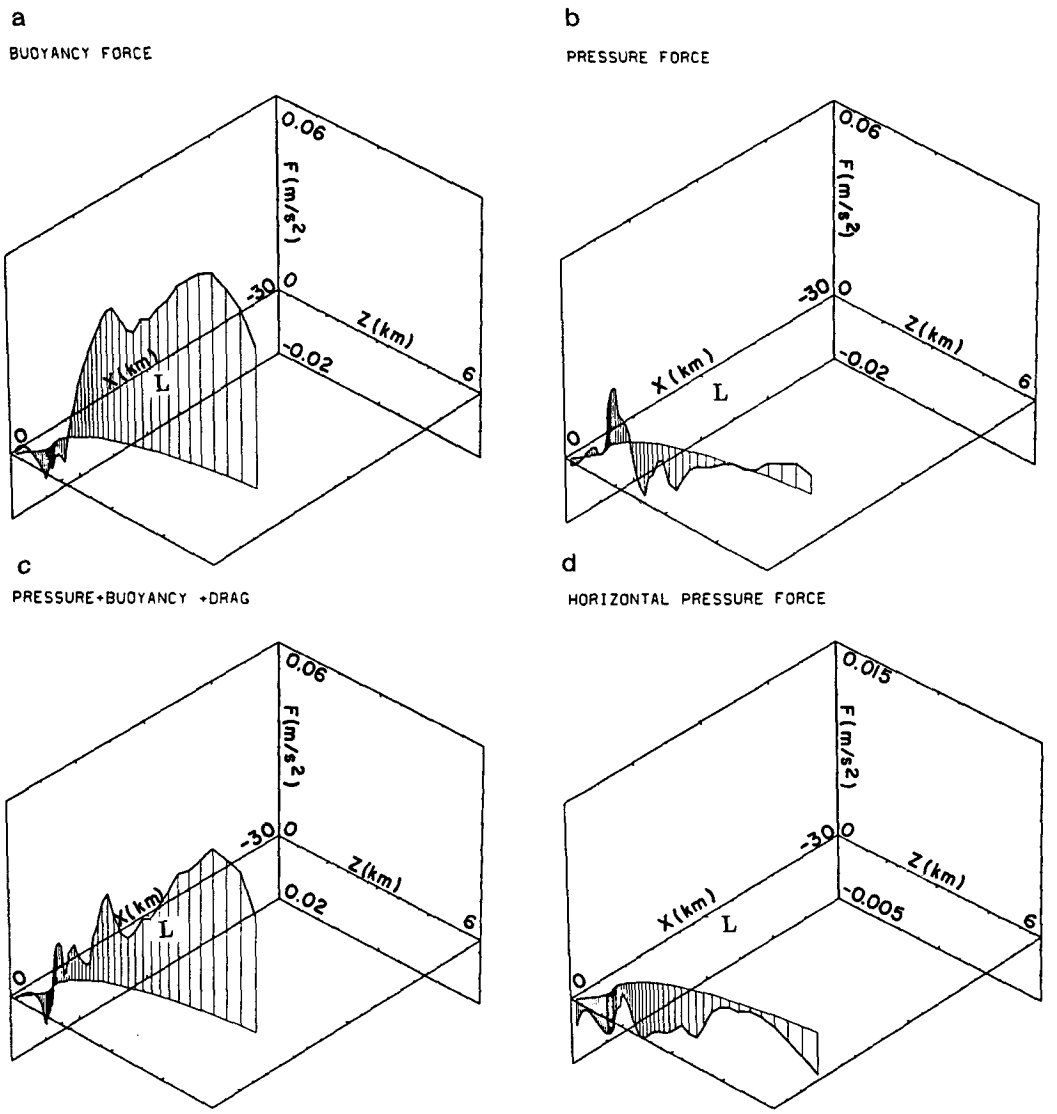

FIG. 2. Forces acting on the parcel which originate at the point $(x_0, z_0) = (-300 \text{ m}, 100 \text{ m})$. (a) buoyancy, (b) vertical pressure gradient, (c) buoyancy + vertical pressure gradient + liquid water drag, (d) horizontal pressure gradient. Note: In Figs. 2–4, fine vertical lines ("fence") indicate time steps and letter L indicates the low center.

2. Description of the calculations

We look at the movement of a Lagrangian parcel in a coordinate system moving with the convective line. The axes are directed as in Part I; i.e., the x-axis is perpendicular to the line and positive in the direction of the line movement and the y-axis is parallel to the line. A parcel accelerates under the influence of gravity, vertical pressure gradient force, and liquid water drag in the vertical direction and horizontal pressure gradient force in the horizontal direction. The two-dimensional pressure field inside the line $P_I(x, z)$ is the sum of the hydrostatic pressure ahead of the line $P_E(z)$ and the pressure disturbance inside the line $p_D(x, z)$. The pressure ahead of the line is given by the environmental sounding (where by environment we mean the environment of the convective line) for the composite, slow moving convective line, from Barnes and Sieckman (1985). The pressure disturbance in the convective part of the line, taken from LeMone et al. (1984), is shown in Fig. 2 of Part I. This pressure disturbance is the result of both hydrostatic and dynamic processes, but according to LeMone (1983) in the case of the slow moving line, it is mainly hydrostatic. She argues that the low pressure behind the leading edge is caused by the presence of warm, humid air above. The position of the low depends hydrostatically on the tilt of the line (see LeMone, 1983). Because the environmental

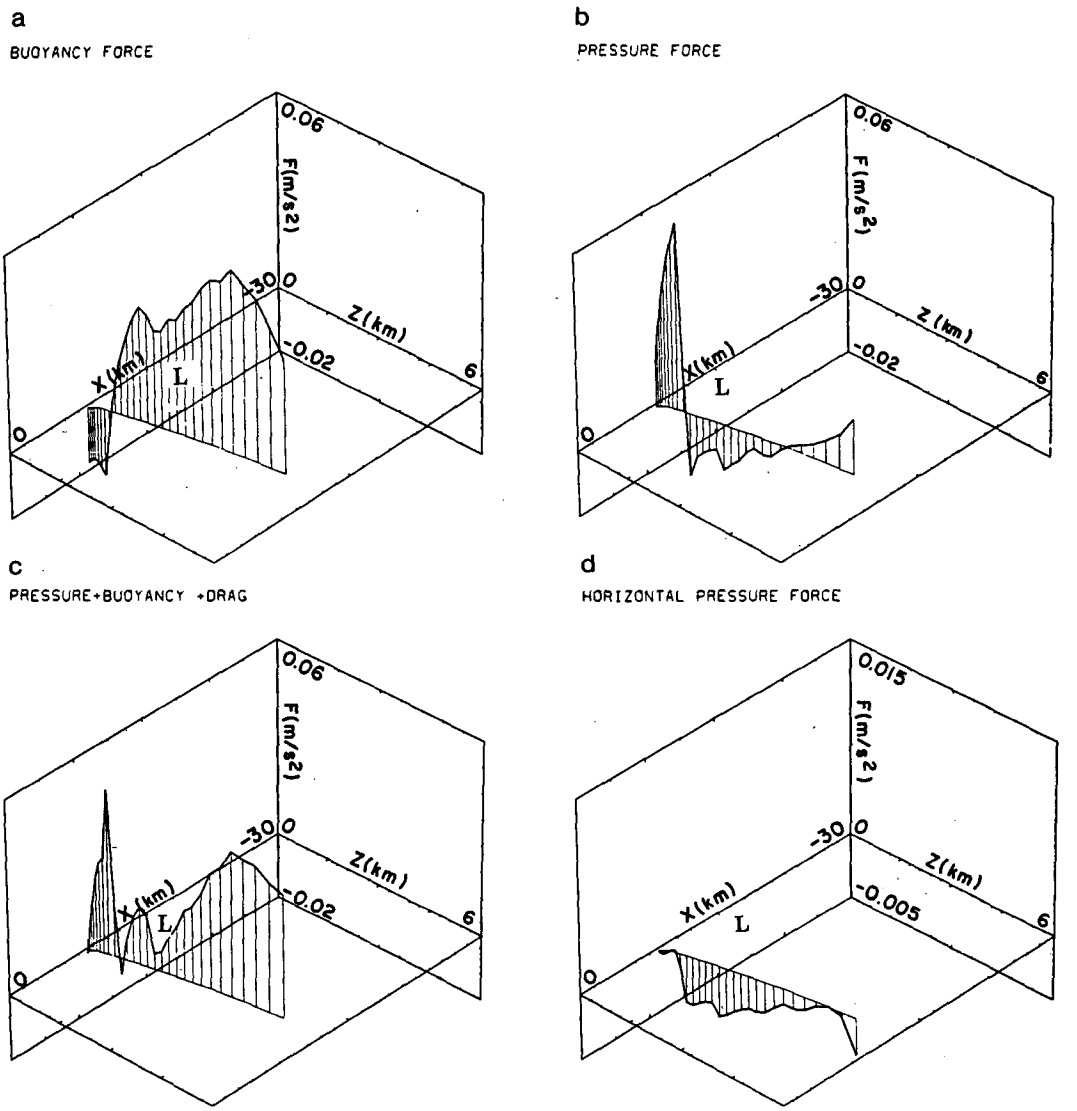

FIG. 3. As in Fig. 2 but originating at the point $(x_0, z_0) = (-8300 \text{ m}, 100 \text{ m})$. (a) buoyancy, (b) vertical pressure gradient, (c) buoyancy + vertical pressure gradient + liquid water drag, (d) horizontal pressure gradient.

pressure $P_E(z)$ is a function of z only, the equation for horizontal velocity u of the parcel takes the form

$$\frac{Du}{Dt} = -\frac{1}{\rho}\frac{\partial p_D(x,z)}{\partial x} + \epsilon u_I(x,z) \qquad (1)$$

where ϵ is the entrainment coefficient and $u_I(x, z)$ is the horizontal velocity of the air mixed into the parcel.

We express vertical forces as the sum of the buoyancy of the parcel relative to the environmental hydrostatic sounding ahead of the line, the disturbance pressure gradient force (containing both hydrostatic and non-hydrostatic effects) and liquid water drag. Therefore, the vertical momentum equation has the form:

$$\frac{Dw}{Dt} = -\left[\frac{1}{\rho}\frac{\partial p_D(x,z)}{\partial z} + \frac{T_p - T_E(z)}{T}g - gq_L\right] \times (1+\alpha)^{-1} + \epsilon w_I(x,z). \qquad (2)$$

In the buoyancy term, T_p is the virtual temperature of the parcel and T_E the environmental virtual temperature ahead of the line.

To make our present results compatible with those of Part I, we calculate mixing with the environment (ϵ), liquid water drag (gq_L) and virtual mass effect [$(1 + \alpha)^{-1}$] using the same values of entrainment, rain efficiency and virtual mass ($\alpha = 0.5$) coefficients as in Part 1. The liquid water drag is calculated with the

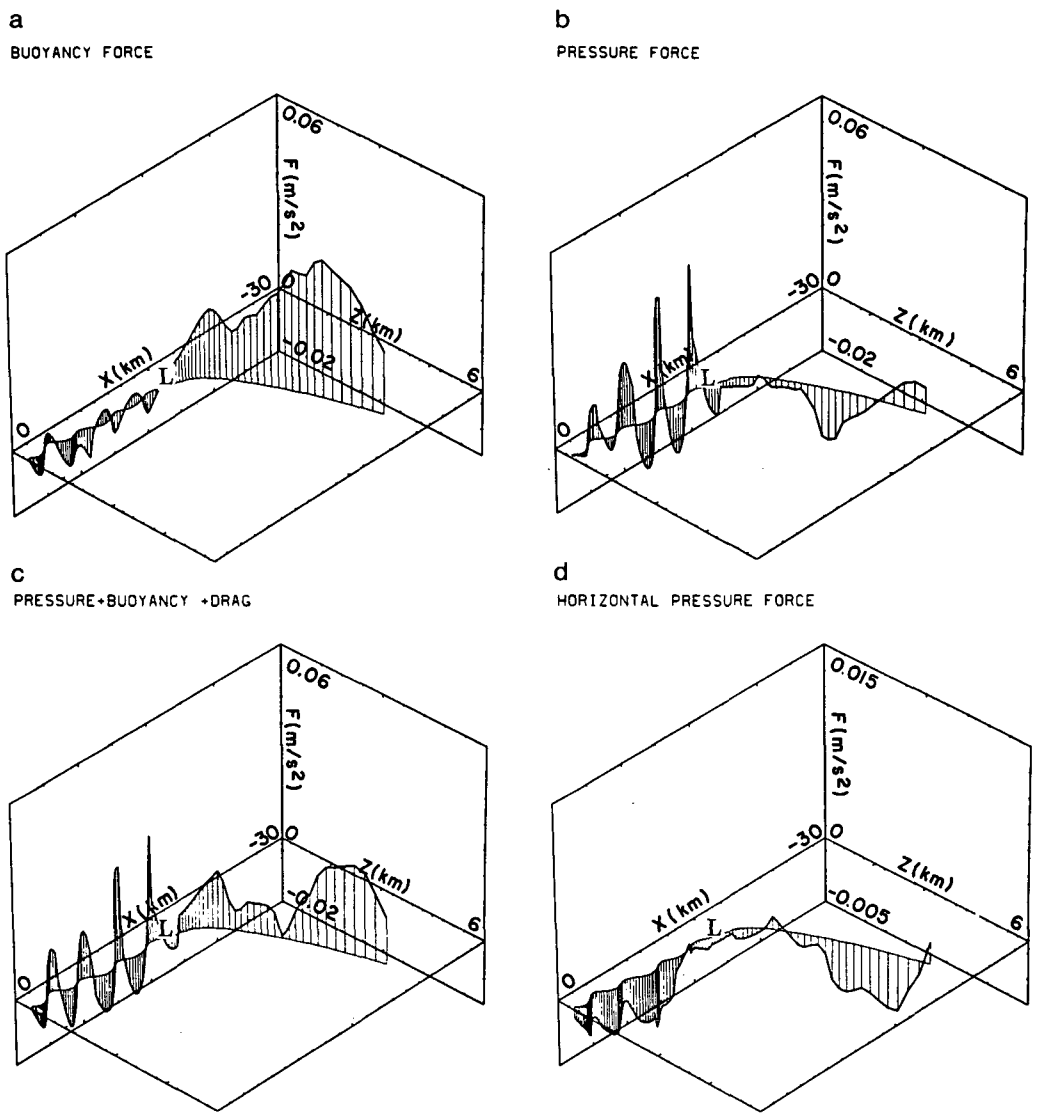

FIG. 4. As in Fig. 2 but originating in the point $(x_0, z_0) = (-300 \text{ m}, 500 \text{ m})$.

assumption that rain efficiency is equal to 0.5 and $q_{L_{max}}$ is equal to 4 g kg^{-1}. Detrainment is neglected and the entrainment of the environmental air causes the mass of the convective parcel to increase linearly up to the cloud top. We assume here that the cloud top is at 12 km and the mass of the parcel at the cloud top is twice its mass at the cloud base. The momentum of the entrained air (u_I and w_I) is obtained from LeMone's (1983) two-dimensional wind fields for the slow-moving convective line. To calculate the temperature of the parcel we assume that the parcel is moving dry adiabatically below the lifting condensation level (LCL) and moist adiabatically above LCL. The temperature of the air mixed into the parcel T_I is calculated as

$$T_I = T_E(z) + T_D(x, z)$$

where T_E is given by the sounding ahead of the line and T_D is calculated from the disturbance pressure field with the assumption that the pressure is hydrostatic (Fig. 1).

Equations (1) and (2) reduce to the momentum equations used in FC parameterization in Part I if we replace the local horizontal pressure gradient $\partial p_D(x, z)/\partial x$ by the grid-averaged pressure gradient calculated separately for updraft and downdraft, neglect the vertical pressure gradient $\partial p_D(x, z)/\partial z$ in Eq. (2), and replace $w_I(x, z)$ and $u_I(x, z)$ by $u_E(z)$ and $w_E(z)$.

We consider Lagrangian parcels originating in the

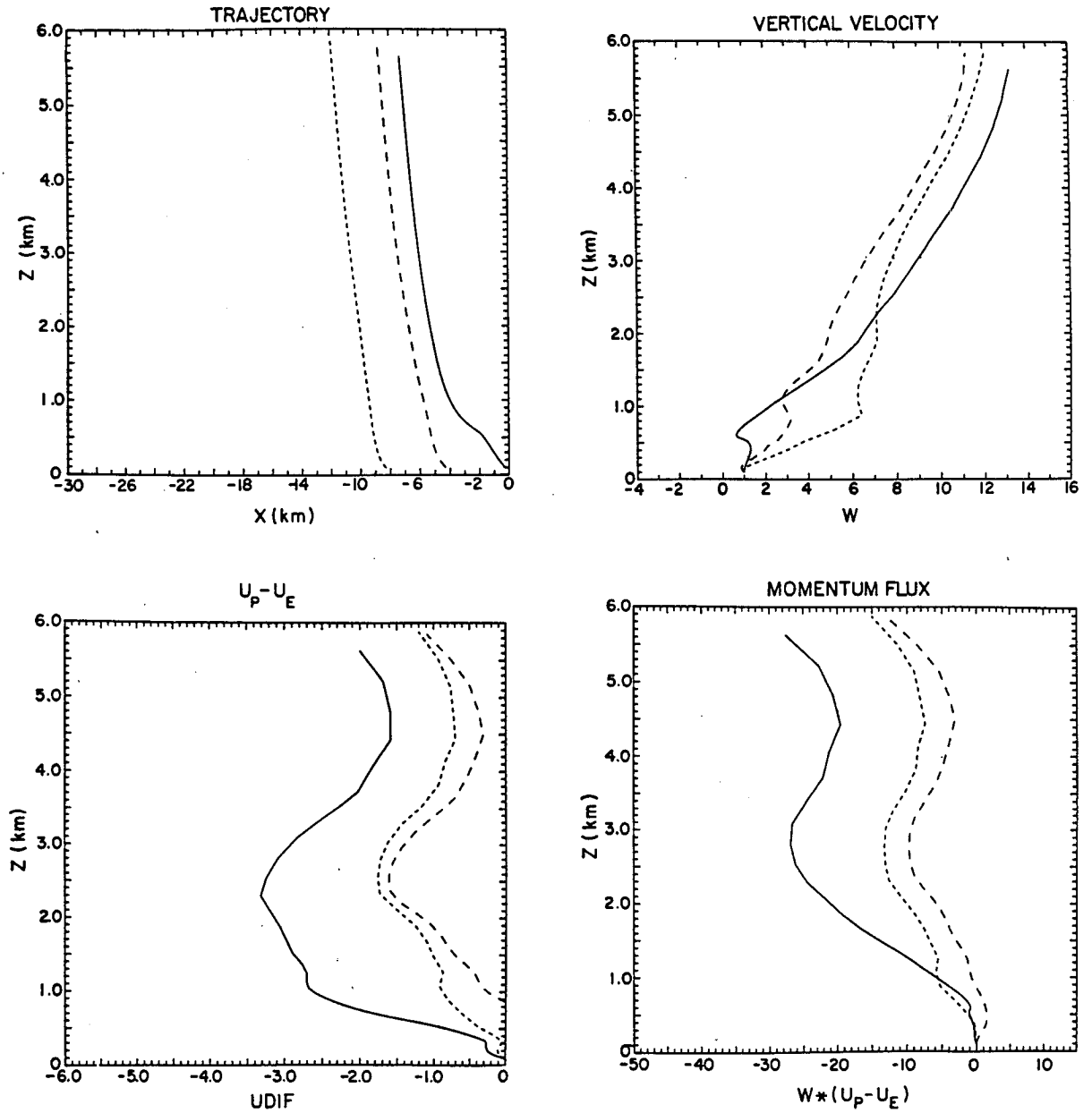

FIG. 5. Examples of trajectories, vertical velocities, momentum ($u_p - u_{EA}$) and momentum fluxes for parcels originating on z_0 = 100 m. Solid lines indicate x_0 = −300 m, coarse dashed lines x_0 = −4300 m, fine dashed lines x_0 = −8300 m.

region of active convection, i.e., at the points (x_0, z_0), where x_0 = −300, −5300, −8300, −12300, −16300 m and z_0 = 100, 200, 300, 400, 500 m. The initial temperature for every parcel is given by $T_I(x_0, z_0)$. As in FC parameterization, the initial vertical velocity is equal to 1 m s^{-1} and the initial horizontal velocity is given by the sounding ahead of the line.

3. Results

The results of our calculations show that the forces acting on the parcel, and consequently its horizontal and vertical momentum, strongly depend on its initial position in the line. Figures 2–4 show examples of vertical and horizontal forces acting on parcels originating at (x_0, z_0) = (−300, 100), (−8300, 100), (−300, 500). The resulting trajectories, velocities and momentum fluxes are displayed in Figs. 5–7. The parcels which originate in the lower layer (100–300 m) and close to the leading edge (Fig. 2) have the highest initial temperature and the greatest buoyancy. As a result, they attain large vertical velocities on the order 14 m s^{-1} (Fig. 5b).

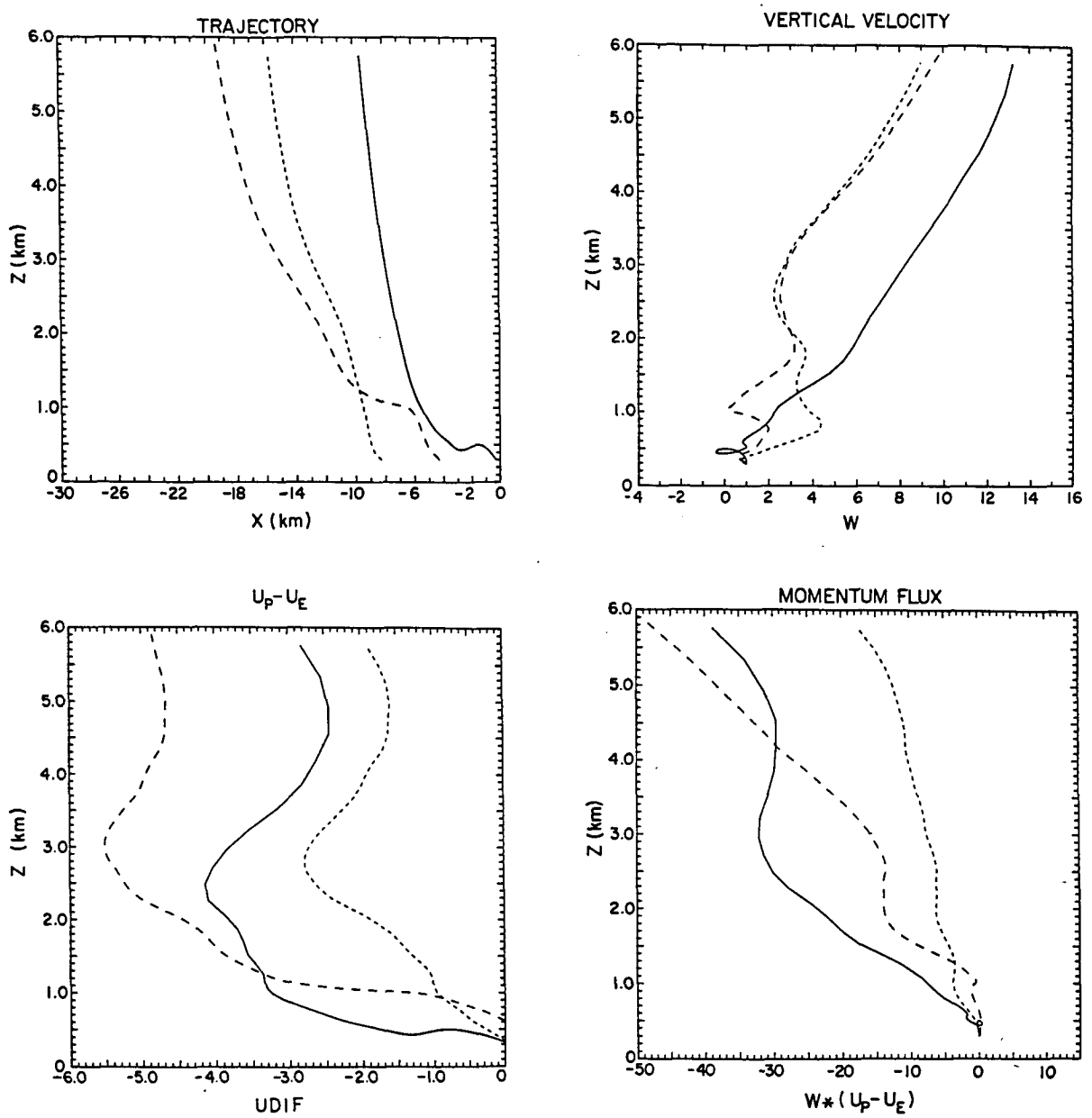

FIG. 6. As in Fig. 5 but for parcels originating on z_0 = 300 m.

Parcels originating in the lower layer but farther from the leading edge (Fig. 3) have a lower initial temperature and smaller buoyancy, but below 1500 m they are accelerated abruptly by a strong vertical pressure gradient force (Fig. 3b). The resulting vertical velocity (Fig. 5b) is large below 1500 m, but increases slowly above 1500 m, and finally reaches values smaller than those for parcels starting close to the leading edge.

The parcels originating higher in the boundary layer (400–500 m) have the smallest buoyancy (Fig. 4a). They move rearward through the line until they are pushed up by the strong vertical pressure gradient near the center of the low (Fig. 4b). They have the smallest vertical velocities. As it can be seen in Fig. 7a, the parcels starting at this level and near the low center (which is located at $x = -10000$ m) oscillate vertically in the boundary layer and never accelerate upward.

The change of parcel momentum caused by horizontal pressure gradients depends on the vertical velocity profile for the parcel, and consequently on its initial position. For example, as can be seen in Fig. 4d, the parcel originating at 500 m near the leading edge

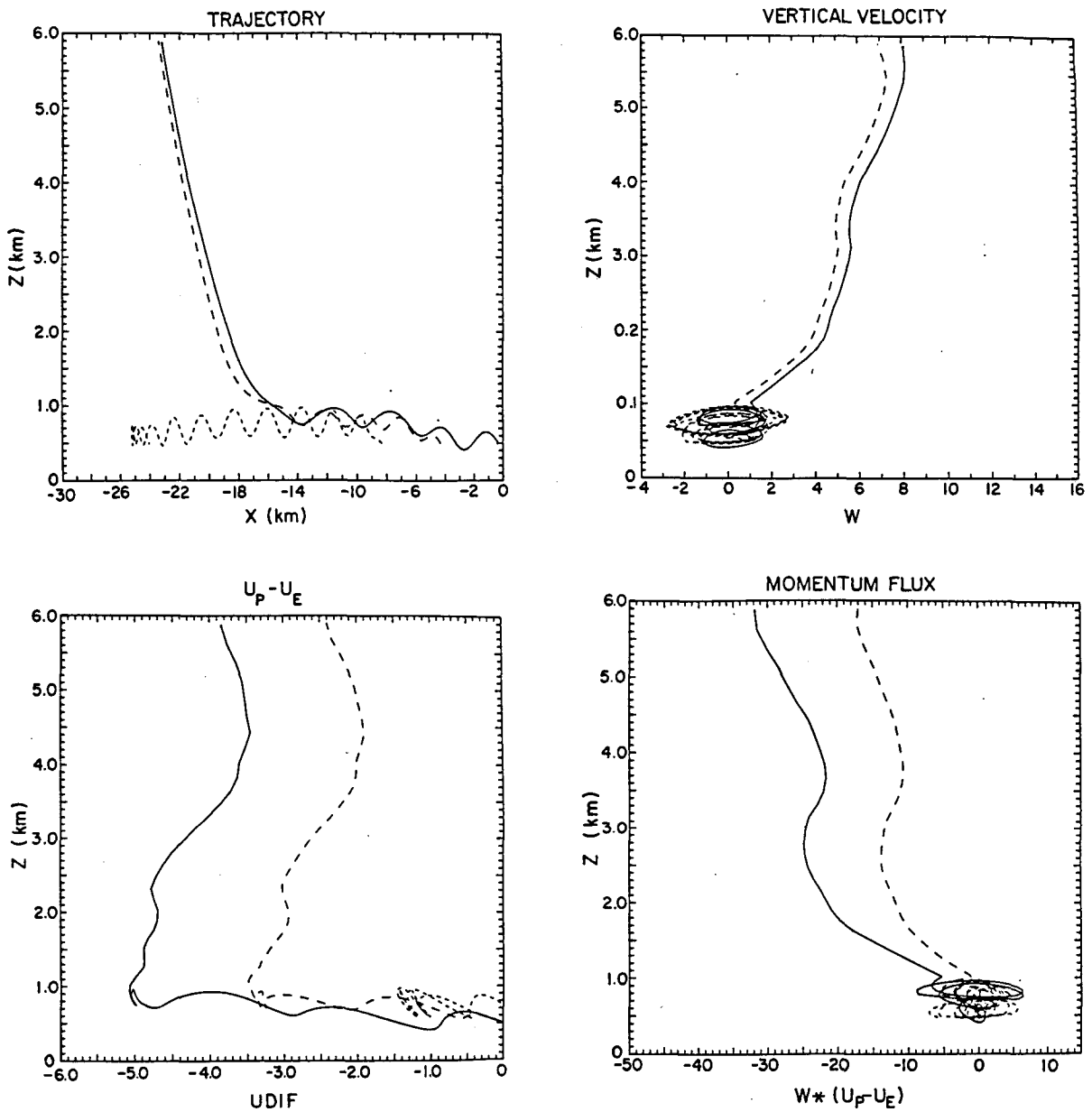

FIG. 7. As in Fig. 5 but for parcels originating at z_0 = 500 m.

remains for a long time in the region with the large horizontal pressure gradient and accelerates strongly rearward (Fig. 7c). Parcels starting at lower levels spend less time under the influence of the large horizontal pressure gradient. Their change in momentum is usually smaller and depends on the distance of the initial position of the parcel from the low center. Parcels starting just slightly forward of the low center ($x_0 = -8300$ m) gain less momentum than parcels originating in the vicinity of the leading edge (Fig. 5c and 6c).

We now determine how the properties of the Lagrangian parcels in our calculations compare to the properties of the convective cores measured in GATE (Zipser and LeMone, 1980). Definition of GATE convective cores is based on aircraft measurements of the vertical velocity. Convective cores are the strongest portions of convective drafts, in which the vertical velocity is larger than 1 m s^{-1} for at least 500 m. Zipser and LeMone measured the average and maximum velocity, diameter and mass flux for every convective core. The statistical distributions of the cores' properties

were then calculated. Following this procedure, we assume that a parcel represents a convective core if its vertical velocity at a given level is larger than 1 m s^{-1}. The main difference between GATE convective cores and our convective parcels lies in the fact that our parcels are represented by points and convective cores by one-dimensional vertical velocity events. Therefore, we cannot calculate a core's diameter and mass flux. Also, although we can describe w in the GATE convective core by $\bar{w}$ and w_{max}, there is only one value of w for our convective parcel. Figure 8 shows that up to 3 km the mean vertical velocity of the Lagrangian parcels is roughly equal to the median w_{max} in the GATE convective cores. At higher levels (above 3 km) average vertical velocity for Lagrangian parcels is larger than the median GATE cores velocity, but it is significantly closer to the observed than the vertical velocity in updraft calculated in the FC parameterization and presented in Fig. 7 of Part I.

Figure 9 displays the effect of horizontal pressure gradients on the momentum flux of the Lagrangian parcels. Momentum fluxes for all the parcels, calculated as $w(u_p - u_E)$, are averaged and multiplied by the fractional coverage of the cores in the convective part of the line using the observational data from Table 3 in Part I. This procedure is used for the cases with and without horizontal pressure gradients.

As in Part I, both momentum fluxes are compared with the momentum flux for the 14 September slow convective line, averaged over the first 30 km behind the leading edge. It can be seen in Fig. 9 that the momentum flux calculated with horizontal pressure gradients agrees extremely well with the observed momentum flux. When the horizontal pressure forces are not included, the calculated momentum flux differs significantly from the observed in both sign and magnitude. These results are consistent with those obtained in the FC parameterization for the slow convective lines.

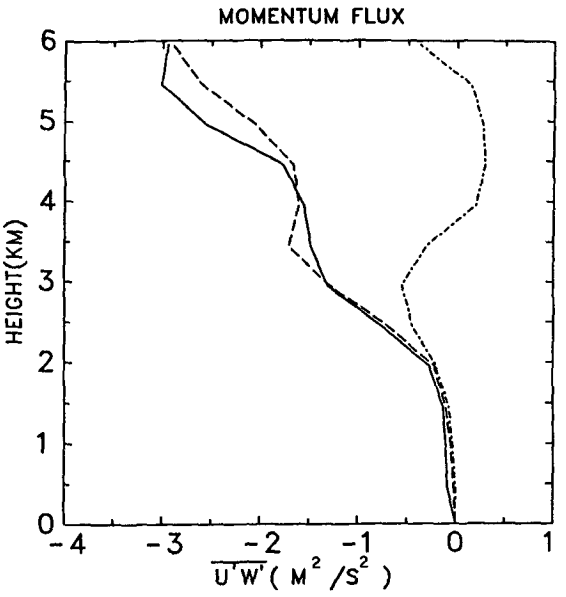

FIG. 9. Comparison of the measured and calculated vertical flux of the horizontal momentum. Solid line: momentum flux for the 14 September convective line averaged over the first 30 km behind the leading edge; Dashed line: average momentum flux for Lagrangian parcels calculated with the horizontal pressure gradients; Dot-dashed line: average momentum flux for the Lagrangian parcels calculated without pressure gradients.

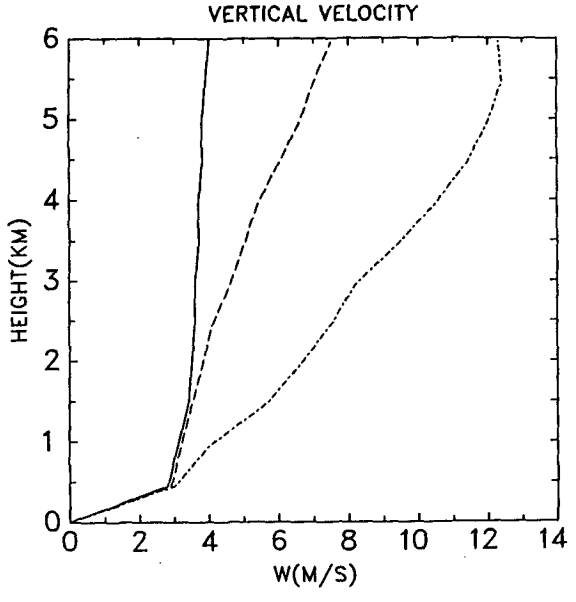

FIG. 8. Comparison of the calculated and measured vertical velocity in the convective cores. Solid line: median w_{max} in GATE convective cores; Dot-dashed line: vertical velocity in the updraft as calculated in FC parameterization in Part I; Dashed line: average vertical velocity for the set of Lagrangian parcels.

4. Conclusions

In this paper we have investigated the influence of the convection-generated pressure field on momentum fluxes in the composite slow-moving GATE convective line. We have shown that the inclusion of horizontal pressure forces in the momentum budgets for Lagrangian air parcels is necessary in order to obtain the realistic magnitude and even the sign of the momentum flux. This independent methodology corroborates the conclusions of Part I, which focused on the dynamic budgets within the FC cumulus parameterization.

Calculations presented in Part I have shown that the effect of horizontal pressure gradient on momentum flux strongly depends on vertical velocity in convective drafts. The FC parameterization overestimated vertical velocity in updraft and downdraft, forcing us to use the observed w in convective drafts in order to obtain realistic momentum fluxes. Here we have shown that

consideration of an ensemble of the convective parcels, moving in the environment modified by convection, significantly improves the calculated vertical velocity. Specifically, the average vertical velocity of an ensemble of convective parcels corresponds much more closely to the average vertical velocity for GATE convective cores than does the vertical velocity of the individual convective parcels. As a consequence, the momentum flux calculations are also improved.

These results allow us to make some suggestions concerning future parameterization of convective momentum fluxes. It was already pointed out by Holton (1973) that including vertical pressure gradients is important for proper vertical velocity calculations. The effects considered by Holton are nonhydrostatic and are often taken into account by the use of virtual mass. The vertical pressure gradients we used in our calculations are predominantly hydrostatic and indicate the temperature changes caused by convection. Positive temperature changes (negative vertical pressure gradient) at the higher levels cause the decrease in parcel vertical velocity. Negative temperature perturbations (positive pressure gradients) close to the surface cause the decrease in the initial temperature of the parcels and consequently, the decrease in their buoyancy and vertical velocity. Since we perform our calculations in the coordinate system moving with the line and assume that in this coordinate system pressure field is stationary, points at different distances from the leading edge correspond to a fixed point on the earth at different times. Therefore, we argue that the application of a time-dependent cloud model with a time-dependent coupling between cloud and mesoscale will significantly improve the vertical velocity and momentum calculations.

Such a parameterization was recently proposed by Pointin (1985), although it was used in a "mesoscale" model with 1.8 km grid resolution and horizontal pressure gradient effects explicitly resolved. Further investigation is required to incorporate the explicit calculation of pressure gradients within the cumulus parameterization itself. In this regard we note that Cho (1985) and Esbensen et al. (1987) have recently discussed alternative formulations of the dynamic interaction between cumulus clouds and their environment.

Acknowledgments. We would like to thank Dr. Margaret LeMone of the National Center for Atmospheric Research (NCAR) and Professor Richard Johnson for their reviews of this research and for helpful and inspiring discussions. We are grateful to Gail Watson carefully typing an earlier draft of this paper, and to our CSU colleagues for editorial assistance. This work was sponsored by the National Science Foundation under Grant ATM-8305759. Computing support was provided by the National Center for Atmospheric Research.

REFERENCES

Barnes, G. M., and K. Sieckman, 1985: The environment of fast- and slow-moving tropical convective cloud lines. *Mon. Wea. Rev.*, **112,** 1782–1794.

Cho, H-R., 1985: Rates of entrainment and detrainment of momentum of cumulus clouds. *Mon. Wea. Rev.*, **113,** 1920–1932.

Esbensen, S. K., L. J. Shapiro and E. I. Tollerud, 1987: The consistent parameterization of the effects of cumulus clouds on the large-scale momentum and vorticity fields. *Mon. Wea. Rev.*, in press.

Fritsch, J. M., and C. F. Chappel, 1980a: Numerical prediction of convectively driven mesoscale pressure systems. Part I: Convective parameterization. *J. Atmos. Sci.*, **37,** 1722–1733.

Holton, J. R., 1973: A one-dimensional cumulus model including pressure perturbations. *Mon. Wea. Rev.*, **101,** 201–205.

LeMone, M. A., 1983: Momentum transport by a line of cumulonimbus. *J. Atmos. Sci.*, **40,** 1815–1834.

——, and E. J. Zipser, 1980: Cumulonimbus vertical velocity events in GATE. Part I: Diameter, intensity and mass flux. *J. Atmos. Sci.*, **37,** 2444–2457.

——, G. M. Barnes and E. J. Zipser, 1984: Momentum flux by lines of cumulonimbus over the tropical oceans. *J. Atmos. Sci.*, **40,** 1815–1932.

Pointin, Y., 1985: Numerical simulation of organized convection. Part I.: Model description and preliminary comparison with squall line observations. *J. Atmos. Sci.*, **42,** 155–172.

Zipser, E. J., and M. A. LeMone, 1980: Cumulonimbus vertical velocity events in GATE. Part II: Synthesis and model core structure. *J. Atmos. Sci.*, **37,** 2458–2469.